Adaptability Analysis of the Drought Monitoring Model based on the Cloud Parameters Method in Africa

Liangming LIU[a], Daxiang XIANG[b]* and Ming LI[c]

a Ph. D, Professor, Ph. D supervisor, Liangming Liu
School of Remote Sensing and Information Engineering
No.129, Luoyu Road, Wuhan, Hubei Province, China
86-27-68778563, 86-27-68778086, lm_liu69@sohu.com

b* Corresponding author.
Ph. D candidate, Daxiang Xiang
School of Remote Sensing and Information Engineering
No.129, Luoyu Road, Wuhan, Hubei Province, China
86-27-68778563, 86-27-68778086, daxiangx@163.com

c Master, Ming Li
School of Remote Sensing and Information Engineering
No.129, Luoyu Road, Wuhan, Hubei Province, China
86-27-68778563, 86-27-68778086, lisouming@163.com

Firstly, the drought monitoring model based on the Cloud Parameters Method/Index (CPI) is briefly introduced in this paper. Meanwhile, the characteristics of the sensor, Spinning Enhanced Visible and InfraRed Imager (SEVIRI), are analyzed from the aspect for drought monitoring. Secondly, we promote a suitable multi-spectral model to detect cloud pixels for the calculation of the three cloud parameters. Then, the drought conditions of Africa in the winter of 2009 and spring of 2010 are monitored by using the cloud parameters method in this paper. Finally, Monthly Evaporation and Monthly Precipitation data from Climate Prediction Center, National Weather Service, US, are taken as reference data to evaluate the drought monitoring result. The comparable analysis indicated that the monitoring results of CPI almost have the same tendency and area as the reference data. Consequently, CPI is adaptable for the drought detecting in Africa.

Keywords: SEVIRI; Cloud Detecting; Drought Monitoring; Adaptability Analysis

1. INTRODUCTION

Drought is not only one of the major natural hazards that bring about billions of dollars in loss to the farming community around the world every year, collectively affecting more people than any other form of natural hazard (Wilhite, 2000 and 2005), but it is also one of the most difficult phenomena to define. In this paper, a broad definition from the National Drought Mitigation Center (NDMC) is accepted: drought originates from a deficiency of precipitation over an extended period of time, usually a season or more, resulting in a water shortage for some activity, group, or environmental sector (NDMC network). Drought should not be viewed as merely a physical phenomenon or natural event. Its impacts on society result from the interplay between a natural event and the demand people place on water supply.

Drought develops slowly, are difficult to detect and have many facets in any single region. The success of drought preparedness and mitigation depends, to a large extent, upon timely information on drought onset, progress and areal extent. These types of information may be obtained through drought monitoring.

The efficiency of a drought monitoring system is deeply influenced by an accurate selection of indices for drought identification, providing a synthetic and objective description of drought conditions. The onset, duration and severity of droughts are often difficult to determine and their characteristics may vary significantly from one region to another (Cooper et al., 2008). Drought monitoring is normally performed using drought indices. Over the years several indices have been developed, each one essentially related to one of the four categories in which the American Meteorological Society has grouped drought definitions and types: meteorological, agricultural, hydrological and socio-economic (Giuseppe M., 2008). Drought indices provide decision makers with information on drought severity and can be used to trigger drought contingency plans, if they are available. The choice of indices for drought monitoring in a specific area should eventually be based on the quantity of climate data available and on the ability of the index to consistently detect spatial and temporal variations during a drought event (Morid et al., 2006).

At present, with the development of information technology, the drought monitoring using remote sensing is advancing and getting maturation. It commonly requires a large time series of multi-spectral data, which including multi-sensor, multi-resolution and multi-scale data (John et al., 2010; Holben et al., 1986). The accurate estimation of regional soil moisture dynamics based on sparse ground measurements is difficult due to soil moisture heterogeneity caused by the spatial heterogeneity of precipitation events, land cover, soil properties, and topography. Now, remote sensing methods for drought monitoring are mainly classified into four categories: Vegetation Index-based (Tadesse et al. 2005; Baigiran et al. 2008), Temperature-based (Jeyaseelan et al. 2008), Vegetation and Temperature-based (Marshall et al. 2004), and Cloud-based (Liu et al. 2007). The representative indices include Vegetation Supply Water Index (VSWI) (Mo W et al. 2006), Temperature/Vegetation Dryness Index (TVDI) (Naira et al. 2007; Patel et al.2009), Apparent Thermal Inertia Index (ATI) (Li et al. 2005; Cai, 2006) and Cloud Parameters Index (CPI) (Liu et al. 2008). This paper mainly introduces the Cloud Parameters Method and analyzes the adaptability of this model in Africa area.

2. STUDY AREA

The case study area, Africa continent, is the world's second-largest and second most-populous continent, with latitude ranged from 35.1S to 37.5N and longitude ranged from 17.7W to 51.6E. At about 30.2 million km² including adjacent islands, it covers 6% of the Earth's total surface area and 20.4% of the total land area. The continent is surrounded by the Mediterranean Sea to the north, both the Suez Canal and the Red Sea along the Sinai Peninsula to the northeast, the Indian Ocean to the southeast, and the Atlantic Ocean to the west.

Africa straddles the equator and encompasses numerous climate areas; it is the only continent to stretch from the northern temperate to southern temperate zones. The climate of Africa ranges from tropical to subarctic on its highest peaks. Its northern half is primarily desert or arid, while its central and southern areas contain both savanna plains and rainforest regions. In between, there is a convergence where vegetation patterns such as Sahel and steppe dominate.

Africa has a long history of rainfall fluctuations of varying lengths and intensities (Nicholson, 1994, 2000). At different spatial and temporal scales, studies showed different behavior of rainfall trends in Africa. Drought has particularly negative impacts on agricultural production in the eastern African region, as most of agriculture is dependent on rainfall (Barron et al., 2003; Slegers, 2008; Thorton et al., 2009).

3. MATERIALS AND METHODS

3.1The SEVIRI Sensor and Data

The second MSG satellite, Meteosat-9, was launched on August 29, 2002 at 3.3 degree West longitude at an altitude of 36,000km. It recorded images of Europe, the North Atlantic and Africa with a temporal resolution of 15min (Coco et al., 2010). The Meteosat Spinning Enhanced Visible and Infrared Imager (SEVIRI) is its main payload, equipped with 12 spectral channels, ranging from visible to thermal infrared wavelengths (Table 1). SEVIRI provides data to the European Organization for the Exploitation of Meteorological Satellites (EUMETSAT) in Darmstadt, Germany. Level 1.5 data were received in compressed form on drivers accessible through personal computers on the network or the DVD media through express delivery.

Table 1. Characteristics of the SEVIRI sensor channels.

Channel	Spectral Range (um)	Centre Spectral (um)	Resolution (km)	Application
1	0.56-0.71	0.635	3	Vegetation
2	0.74-0.88	0.81	3	
3	1.50-1.78	1.64	3	
4	3.48-4.36	3.92	3	
5	5.35-7.15	6.25	3	Water vapor
6	6.85-7.85	7.35	3	
7	8.30-9.10	8.70	3	
8	9.38-9.94	9.66	3	
9	9.80-11.80	10.80	3	
10	11.00-13.00	12.00	3	Temperature
11	12.40-14.40	13.4	3	
12	0.50-0.90	0.75	1	HRV

As same as the other sensors, the coarse spatial resolution of SEVIRI data, equal to 3 km at the sub-satellite point, introduces further spatial uncertainties due to the mixture of land cover elements (Coco et al., 2010). The high temporal frequency of SEVIRI data increases the chance to obtain land surface information (Fensholt et al., 2006). In this study, channels one (visible, 0.56 - 0.71um), two (near infrared, 0.74 - 0.88um), three (short wave infrared, 1.50 - 1.78um), and ten (thermal infrared, 11.00-13.00um) which are converted to reflectance and bright temperature have been used to detect the cloud. We used images covering the region during May, 2009 to April, 2010, recorded between 12:00 and 13:00 local time.

3.2 Method

3.2.1 RS Data Preprocessing

The preprocessing operations mainly include calibration and re-projection. Calibration processing converts the original Digital Number to reflectance or bright temperature through slope-intercept form with revised solar altitude and Earth-Sun Distance at the imaging moment. And the calibration information, including slope and offset, could be read from the image header information. The re-projection changes the satellite orbit projection to the geographic (latitude/longitude) projection by strict transformation calculation method in order to correct the every pixel's geometric location.

In our research team, a tool of an operational MSG SEVIRI processor has been built in VC++. Outputs from the tool are reflectance in channels 1, 2 and 3 of Level 1.5 MSG SEVIRI data. Meanwhile, the tool also handles the thermal infrared channels for retrieve the bright temperature. The products from the processor are composed of 2776 by 2904 pixels with 0.025 latitude/longitude resolution for all channels except HRV.

3.2.2 Multi-spectral cloud detection method

In the field of remote sensing application, cloud detecting is a preliminary important operation in most algorithms for processing radiance data measured from sensors onboard satellites, because the sensor cannot scan the land surface as a result of the coverage of cloud. Nevertheless, cloud is an important information source for our drought monitoring model. Consequently, a high quality cloud detection algorithm is also needed in order to monitor drought well.

Clouds are generally characterized by higher reflectance and lower temperature than the underlying land surface. But there are many surface conditions when this characterization of clouds is inappropriate and some cloud types are difficult to be detected because of insufficient contrast with the surface radiance (Amato et al., 2008). For example, in the visible channel, the apartment between desert and cloud is a difficult problem because the desert has the same reflectance characteristic with cloud, especially in the junction of cloud and desert edges. Many of these concerns can be mitigated by multispectral approaches to cloud detection and, for this reason, the availability of multispectral sensors, able to measure radiance emitted by land surface at several and narrow spectral bands, represents an important improvement in this field (Yang et al., 2006).

At present, most of multispectral cloud detection methods are based upon the spectral behavior of clouds both in the emissive infrared and reflective channels. Generally some decision rules are set involving a few selected spectral channels; then thresholds on the value of radiances are empirically chosen to discriminate between the cloudy and clear sky conditions.

In this study, a new multispectral cloud detection method for SEVIRI images is conducted after analyzing the multispectral characteristics of cloud and land cover (vegetation and desert). The spectral curves were drawn on each day at 12:12 a.m (UTC) in the following figures:

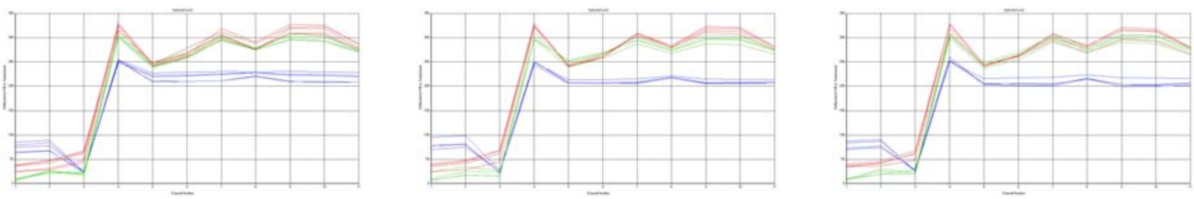

(a) 1st May 2009 *(b) on 1st July 2009* *(c) 1st September 2009*

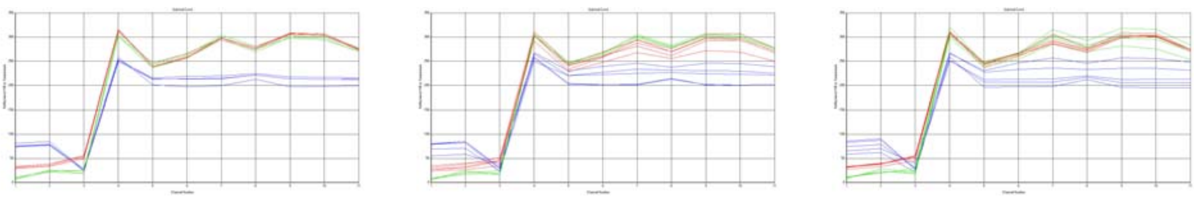

(e) 1st November 2009 *(f) on 1st December 2009* *(g) 1st February 2010*

Figure 1. Spectral curves of typical objectives (blue lines: cloudy pixels, red lines: desert pixels and green lines: other land covers).

From the above figures, in the two visible channels and the short wave infrared channel, there are relatively obvious differences during the reflectance characteristics of desert, cloud and vegetation. In the visible channels, the cloud reflectance is higher than that of land surface cover. However, the cloud edge and desert edges maybe have the same reflectance, thus an absolute sleeping threshold principle is not adapted for the apartment between them. A sharp decrease between the reflectance of infrared and short wave infrared when the cloudy pixels, while it was low decrease when clear sky pixels except desert. In addition, the reflectance of short wave infrared channel is higher than that of infrared channel when desert. Thus, the signed of reflectance slope can be considered as an index to separate desert coverage. In the IR12.0 (channel 10), the bright temperatures of clear sky pixels are higher than cloud pixels. Therefore, the bright temperature could be taken as an index to discharge the cloud and clear sky pixels. In conclusion, the cloud detection method can be established by the following formula:

$$CI = \sum_{i=1}^{3} \varepsilon(f_i) = \varepsilon(R_1 - TH_{R_1}) + \varepsilon(R_2 - R_3) + \varepsilon(TH_{T_{10}} - T_{10}) \tag{1}$$

$$\varepsilon(f) = \begin{cases} 0, & \text{if } f \le 0, \\ 1, & \text{otherwise.} \end{cases} \tag{2}$$

Where R_i is the reflectance of channel i (i=1,2 and 3); T_{10} is the bright temperature of channel 10; $\varepsilon(f)$ is step function; TH_{R_1} and $TH_{T_{10}}$ are sleeping thresholds for channel 1 reflectance and channel 10 bright temperature respectively. The two thresholds will be influenced by the change of seasonal, listed in Table 2.

In the above formula, we can find that the index is equal to 3 if cloudy pixel because of its characteristics of higher reflectance in visible channel, lower reflectance in short wave channel and lower temperature in thermal infrared channel.

3.2.3 Cloud parameters method

The shape of cloud parameters method was selected on the basis of the following prerequisites: (1) No cloud indicates no precipitation, and increased possibility of drought; (2) No cloud indicates strengthened solar radiation at shortwave, more transpiration and increased possibility of drought. These two prerequisites are fundamentally generalized from law of nature (Tan et al., 2004).

The three cloud parameters, which are the core parameters of CPI, are defined to demonstrate information described by cloud: in a monitoring period, Continuous Cloud-Free Days (CCFD) which refers to the longest days of the study site with no cloud continuously, Cloud Days Ratio (CDR) which refers to the ratio between summary days with cloud and summary days, and Continuous Cloud Days (CCD) which refers to the longest days of the study site covered with cloud continuously. With three cloud parameters calculated, relationship between these indexes and drought condition could be generalized as functions, which are finally combined to show the Cloud Parameters Method Index (CPI) as the following formula (Liu et al., 2008):

$$CPI = \frac{F_1 \cdot W_1 + F_2 \cdot W_2 + F_3 \cdot W_3}{F_1 + F_2 + F_3} \tag{3}$$

Here, W is the infection function and is F weight.

As a general knowledge, the solar radiation reaching the top of the atmosphere mainly depends on the relative space position and the moving laws between the sun and the earth. The solar radiation received per units of area and time is varied, which mainly owing to the differences of seasons, moments, latitude, atmospheric transparency and altitude. The space and time distributions of solar radiation are determined by the distance of the earth from the sun, the altitude of the sun and the duration of the sunshine (Liu et al., 2008).

Consequently, temporal and spatial changes will lead to diversity of drought conditions. For example, for the same place at different seasons, the same cloud indexes might indicates different conditions of soil moisture, due to different solar zenith angles, received solar radiance and intensity of transpiration. With the same consideration as temporal change, spatial change will also affect the contribution made by cloud indexes for drought condition, so quantitative method is also applied to analysis and modify the infection functions. However, in the original cloud parameters method model, the drought index has nothing to do with temporal and spatial change; it is only affected by the values of three cloud parameters. So it is required to perform naturalization for these infection functions, which lead to the improved cloud parameters method. With temporal and spatial modification applied, three basic infection functions could be rewritten as the following formula:

$$W = P(CI, Q, P) \tag{4}$$

Here: W is the modified (naturalized) infection function, P is the basic function, Q is the modification function for CCFD, CCD, CDR with spatial changes, while R is the modification function for CCFD, CCD, CDR temporal changes. The CI (cloud indexes) indicates CCFD, CCD and CDR respectively.

3.2.4 Adaptability analysis

In the cloud parameters method model, the precipitation and the evaporation are considered to the input and output of the whole earth system. Consequently, the difference between them can correctly describes the soil moisture conditions, that is to say, we can take this difference as the actual soil humidity to evaluate the result of cloud parameters method drought monitoring. In this study, monthly evaporation and precipitation data, received from Climate Prediction Center, National Weather Service (NWS, network), US, are taken as reference data to evaluate the drought monitoring result.

For the monthly evaporation and precipitation data, they have the same units, millimeter per month (mm/mon), thus the difference between them can be directly calculated. In generally condition, the drought pressure will increase with the decreased of the difference (ΔD_{pe}), and it is vice versa. In addition, the drought conditions of current monitoring period could be affected by the last one in a certain extent. So, the Reference Drought Index (RDI) indicated drought condition can be established by the following formula:

$$RDI = f(\Delta D_{pe\_cur}, \Delta D_{pe\_his}) = a * \Delta D_{pe\_cur} + b * \Delta D_{pe\_his} + c \tag{5}$$

Where ΔD_{pe_cur} is the current monitoring period difference, ΔD_{pe_his} is the latest one, a , b and c are coefficients.

4. RESULTS

This section shows the experiments worked out on the method of Section 3. It mainly includes cloud detecting, drought monitoring and adaptability analyzing.

4.1 Cloud detecting

From the figure 1, we can see that the reflectance and temperature are influenced by the change of seasonal. Consequently, in order to improve the accuracy of cloud detecting, the absolute sleeping thresholds should be modified at a certain extent. After many experiments, the following thresholds table was established for the reflectance and bright temperature:

Table 2. Thresholds of reflectance and bright temperature.

Year	2009								2010			
Month	May	Jun.	Jul.	Aug.	Sept.	Oct.	Nov.	Dec.	Jan.	Feb.	Mar.	Apr.
TH_{R_1}	0.28	0.30	0.30	0.30	0.28	0.28	0.28	0.25	0.25	0.25	0.28	0.28
$TH_{T_{10}}(K)$	275	280	280	280	275	275	275	270	270	270	275	275

The influence by the seasonal changing can be seen with half an eye from the table. The reflectance and temperature thresholds reach to the peak value in summer, while they arrive at the bottom value in the winter.

Based on the multispectral cloud detection algorithm from the formula (1), the results of cloud detecting were drawn in the following figure:

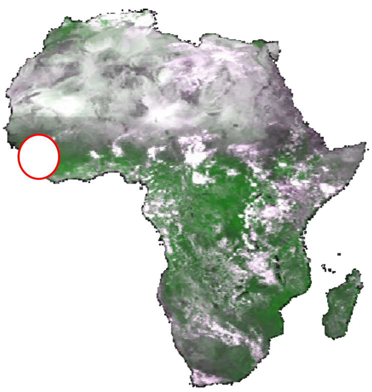

(a) 1st May. 2009(true colors: red, infrared, red)

(b) cloud detecting result of1st May. 2009

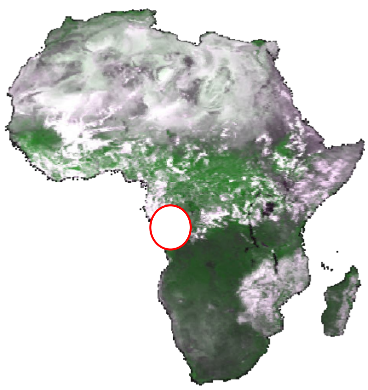

(c) 1st Jul. 2009(true colors: red, infrared, red) *(d) cloud detecting result of1st Jul. 2009*

Figure 2. Result of cloud detecting.

From the figures, the accuracy of cloud detecting is mostly preferable and usable. However, the reflectance and temperature of edged cloudy pixels are affected by the corresponding land cover, such as the red circle regions in figure (a) and (c). That is to say, the energy which remote sensing detector received contains that of cloud and land cover when thin cloud or fragmented. Therefore, the influence of land cover should be considered as an important element in cloud detection method in the future study.

4.2 Drought Monitoring and Adaptability Analyzing

During the procession of drought monitoring, one month was taken as monitoring period in order to meet the model's requirement. After cloud detecting, the three cloud parameters were calculated by statistical method from the serial cloud result in each monitoring period. Then, the three cloud parameters were applied into the drought monitoring model with the temporal and spatial modifications.

The reference data are the monthly evaporation and precipitation obtained from the Climate Prediction Center, National Weather Service, US. The raw data cover the global and are JPEG format. Before applied to evaluate drought monitoring results, these data were operated by geometric correction and extracting interested region.

The drought condition (figure 3 (a)) which retrieved from the remote sensing images and the reference data (figure 3 (b), (c), (d), (e)) are listed in the following figure:

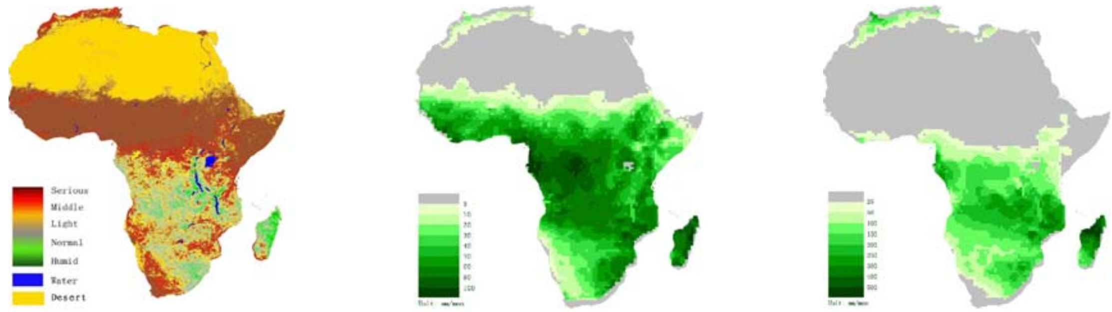

(a) Drought of Jan. 2010 *(b) Evaporation of Jan. 2010* *(c) Precipitation of Jan. 2010*

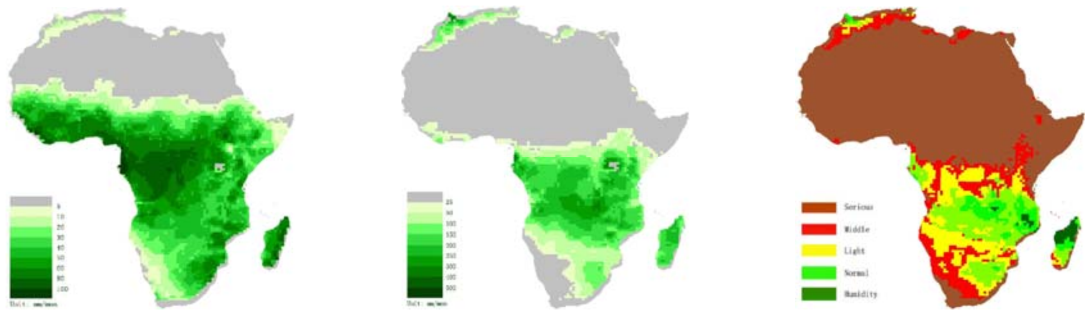

(d) Evaporation of Dec. 2009 *(e) Precipitation of Dec. 2009* *(f) Result of Jan. 2010 from Dpe.*

Figure 3. Result of drought monitoring.

According to the formula (5), differences of Dec. 2009 and Jan. 2010 should be calculated in order to evaluate the accuracy of drought monitoring result from the cloud parameters method on Jan. 2010. However, the drought condition of the current monitoring period is affected by that of history because drought is a durable procession. In addition, the influence extent directly relates with the drought condition. Thus the coefficients are variety with the relationship of current and history drought conditions. In our experiments, the values of the three coefficients are listed in the following table:

Table 3. Values of three coefficients: (a,b,c).

History \ Current	Serious	Middle	Light	Normal	Humidity
Serious	(0.60,0.40,0.00)	(0.73,0.27,0.00)	(0.86,0.14,0.00)	(0.85,0.15,0.00)	(0.75,0.25,0.00)
Middle	(0.69,0.31,0.00)	(0.60,0.40,0.00)	(0.71,0.29,0.00)	(0.78,0.22,0.00)	(0.71,0.29,0.00)
Light	(0.83,0.17,0.00)	(0.73,0.27,0.00)	(0.60,0.40,0.00)	(0.68,0.32,0.00)	(0.68,0.32,0.00)
Normal	(0.76,0.24,0.00)	(0.81,0.19,0.00)	(0.71,0.29,0.00)	(0.60,0.40,0.00)	(0.65,0.35,0.00)
Humidity	(0.72,0.28,0.00)	(0.89,0.11,0.00)	(0.86,0.14,0.00)	(0.68,0.32,0.00)	(0.60,0.40,0.00)

From the table, it is obviously seen that the extremities of history drought condition, serious and humidity, are more severely influencing the current drought condition than other drought grades. The figure 3(f) was calculated according to formula (5) based on the coefficients' value in Table3.

Comparing the remote sensed monitoring result (figure 3(a)) and the reference result (figure 3(f)), the whole drought condition trends between them are similar with each other. The concrete accuracy of drought condition Jan. 2010 is listed in the following table:

Table 4. Evaluate accuracy (%).

Reference \ RS	Serious	Middle	Light	Normal	Humidity	Producer accuracy
Serious	51.0331	8.3125	5.1753	2.8665	0.1060	75.6120
Middle	1.4135	5.6399	6.5661	5.8989	0.3727	28.3539
Light	0.6472	1.6171	2.4928	4.4282	0.5880	25.5060
Normal	0.1776	0.1993	0.3117	1.2801	0.4340	53.2765
Humidity	0.0439	0.0275	0.0196	0.2211	0.1275	29.0111
User Accuracy	95.7194	35.7039	17.1143	8.7112	7.8316	Acceptable: 83.8775

The definition of the acceptable accuracy is that the difference of grade results is lower than one level. From the accuracy table, the acceptable accuracy is as high as 83.8775%. However, the producer and user accuracies are too low, such as the user accuracies are 8.7112% and 7.8316% in Normal and Humidity conditions, respectively. This phenomenon may be caused by the drought conditions classification error of reference data. Thus, the classification of reference data is a focus problem in our future research.

5. CONCLUSIONS

The present paper demonstrated very good adaptability of the cloud parameters method over Africa area from multispectral remotely sensed images taken from radiometers onboard geostationary satellites, precisely SEVIRI on-board MSG. Where, reliability of the multispectral cloud detection method ranged from good to excellent in all analyzed conditions (four seasons). The results of cloud detecting and drought monitoring were achieved resorting to some remote sensed image procession tools (namely, ERDAS and ENVI) able to exploit multispectral character of the sensor at best.

Firstly, even though same robustness is guaranteed by the statistical character of the cloud detection method and by choosing only pixels estimated confidently clear or cloudy for the training phase, however particular conditions, as light clouds, cloud deserve more attention. In practice it is expected that the training information has a seasonal and geographical variation mainly due to the varying spectral characteristics of the underlying surface (vegetation, especially). We can easily find that the cloud detection method in this paper contains two types of sleeping thresholds which varieties with seasonal changes were applied and the detecting results rely on the types of land cover. Thus, further improvement of the methodology can be obtained by resorting on dynamic thresholds rather than sleeping ones and types of land surface cover. That is to say, a new operative algorithm with relationship of temporal and spatial dynamic thresholds should apply to detect cloud in the future study.

Secondly, the drought monitoring model can be considered fully integrated physical/statistical, where the link with physics is guaranteed by the use of a much consolidated drought condition to train the discriminated analysis by the monthly precipitation and evaporation data. Several months have to be addressed in order to evaluate accuracy of the drought monitoring further, and the relatively accuracy reach as high as 83.8775%. Consequently, the drought monitoring model based on the Cloud Parameters Method is adaptable for the drought detection in Africa. What's more important is to offer a new drought monitoring method with high accurate and adaptable to the drought field in Africa. However, verification of the two important problems, the stability of the cloud parameters method in Africa area and the availability of business operations in routine works, is an urgent task.

REFERENCES FROM JOURNALS:

Amato U., Antoniadis A., Cuomo V., Cutillo L., Franzese M., Murino L., Serio C., 2008, Statistical cloud detection from SEVIRI multispectral images, Remote sensing of Environment, 112, 750-766.

Baigiran P.R., Darvishsefat A.A., Khalili A., 2008, Using AVHRR-based vegetation indices for drought mobitoring in the Northwest of Iran, Journal of arid environments, 72, 1083-1093.

Barron, J., Rocksto¨m, J., Gichuki, F., Hatibu, N., 2003, Dry spell analysis and maize yields for two semi-arid locations in east Africa, Agriculture and Forest Meteorology, 17, 23–37.

Coco M.R., Wietske B., Alfred S., 2010, Image mining for drought monitoring in eastern Africa using Meteosat SEVIRI data, International Journal of Applied Earth Observation and Geoinformation, 12,63-68.

Cooper, P., Dimes, J., Rao, K., Shapiro, B., Twomlow, S., 2008, Coping better with current climatic variability in the rain-fed farming systems of sub-Saharan Africa: an essential first step in adapting to future climate change? Agriculture, Ecosystems & Environment, 126 (1–2), 24–35.

Fensholt R., Sandholt I., Stisen S., Tucher C., 2006, Analysing NDVI for the African continent using the geostationary meteosat second generation SEVIRI sensor, Remote sensing of environment, 101, 212-229.

Giuseppe M., Alfonso S., Pasquale V., 2008, A groundwater resource index for drought monitoring and forecasting in a Mediterranean climate, Journal of Hydrology, 357, 282-302.

Holben B., Fraser R., 1984, Red and near-infrared sensor response to off-nadir viewing, International Journal of Remote Sensing, 5(1), 145−160.

Jeyaseelan A.T., Kogan F.N., 2008, Evaluation of GVI based indices for drought early warning in India, Disaster forewarning diagnostic methods and management, 6412, 4120-4120.

John D., Wade T., Xiwu Z., Thomas J. Curt A., 2010, Evaluating the utility of Remotely Sensed soil moisture retrievals for operational agricultural drought monitoring, IEEE Journal of Selected Topics in Applied Earth Observations and Remote Sensing, 3, 57-66.

Li W., Mao S.Y., Chen W., 2005, A new method of cloud detection in MODIS image, Conference proceedings of the seventh international conference on electronic measurement and instruments, 7, 281-285.

Liu L.M., Xiang D.X., Zhou Z., Dong X.Y., 2008, Analyses the modification functions of the drought monitoring model based on the cloud parameters method, The 2008 international congress on image and signal processing, 687-691.

Liu L.M., Xiang D.X., Dong X.Y., 2007, Improvement of the drought monitoring model based on the cloud parameters method and remote sensing data, International workshop on knowledge discovery and data mining, 293-296.

Marshall G., Zhou X.B., 2004, Drought detection in semi-arid regions using remote sensing of vegetation indices and drought indices, IEEE international geo-science and remote sensing symposium proceedings, 1555-1558.

Mo W, Wang Z, Sun H, Ma L, He L, 2006, Remote Sensing Monitoring of Farmland Drought Based on Vegetation Supply Water Index, Journal of Nanjing Institute of Meteorology, 29(3), 396-401.

Morid S., Smakhtin V., Moghaddasi M., 2006, Comparison of seven meteorological indices for drought monitoring in Iran, International journal of climatology, 26, 971-985.

Naira C., Robert L., Ramata M., Marouane T., 2007, Surface soil moisture status over the Mackenzie River Basin using a Temperature/Vegetation index, International geo-science and remote sensing symposium, 12, 1846-1848.

Nicholson, S., 1994, Recent rainfall fluctuations in Africa and their relationship to past conditions over the ontinent. The Holocene 4, 2, 121–134.

Nicholson, S., 2000, The nature of rainfall variability over Africa on time scales of decades to millennia, Global and Planetary Change, 26, 137–158.

Patel N.R., Anapashsha R., Kumar S., Saha S.K., Dadhwal V.K., 2009, Assessing potential of MODIS derived temperature/vegetation condition index(TVDI) to infer soil moisture status, international journal of remote sensing, 1, 23-29.

Slegers, M., 2008, ‘‘If only it would rain’’: farmers’ perceptions of rainfall and drought in semi-arid central Tanzania, Journal of Arid Environment, 72, 2106–2123.

Tadesse T., Brown J.F., Hayes M.J., 2005, A new approach for predicting drought-related vegetation stress: integrating satellite, calimate, and biophysical data over the US central plains, ISPRS journal of photogrammetry and remote sensing, 59, 244-253.

Tan D.B., Liu L.M., Yan J.J., 2004, Study of drought monitoring model based on MODIS data, Journal of Yangtze River Scientific Research Institute., 3, 11-15.

Thorton, P., Jones, P., Alagarswamy, G., Andresen, J., 2009, Spatial variation of crop yield response to climate change in East Africa, Global Environmental Change, 19, 54–65.

Wilhite, D.A., 2000, Drought as a natural hazard: Concepts and definitions, In: Wilhite, D.A.(Ed.), Drought: A global assessment, Hazards Disaster Ser., 1, 3-18.

Yang, Y., Lin, H., Jiang, J., 2006, Cloud analysis by modeling the integration of heterogeneous satellite data and imaging, IEEE Transactions on Systems, Man and Cybernetics — Part A: Systems and Humans, 36, 162−172.

EFERENCES FROM BOOKS:

Cai G., 2006, MODIS data based thermal inertia and land surface temperature modeling and their applications in determination of soil moisture and heat exchange, doctoral dissertation, Institute of remote sensing applications Chinese academy of sciences.

Wilhite, D.A., 2005, Drought and water crisis: science, technology and management issues. Taylor & Francis Group.

EFERENCES FROM INTERNET:

Africa, from Wikipedia, the free encyclopedia: http://en.wikipedia.org/wiki/Africa#Geography.

NDMC, National Drought Mitigation Center: http://drought.unl.edu/.

NWS, National Weather Service: http://www.cpc.ncep.noaa.gov/cgi-bin/gl_Soil-Moisture-Monthly.sh#

ACKNOWLEDGEMENTS:

This paper is supported by the Special Study of the Risk Communication Technologies on Key Technologies for Natural Disaster Risk Prevention of Natural Disaster (2008BAK50B08-03), the Project in the National Science & Technology Pillar Program during the Eleventh Five-Year Plan Period of China. The authors thanks EUMETSAT to provide SEVIRI data, and also thanks Climate Prediction Centre, National Weather Service, to provide Monthly evaporation and precipitation data.

AUTHOR BIOGRAPHY:

Liangming LIU received the B. S. degree in Geo-Information Engineering from Wuhan Technical University of Surveying and Mapping (WTUSM) in 1992 and the M. S. and Ph. D. degrees in Photogrammetric and Remote Sensing from Wuhan University in 1999 and 2004 respectively. He is currently the Professor at School of Remote Sensing and Information Engineering, Wuhan University, Wuhan, Hubei Province, China. His research activities involve: processing and analysis of satellite data, application of remote sensing and GIS technology in field of natural disaster and environment. He founded and is the Chief of Institute of Remote Sensing for Environment and Disaster in Wuhan University.

Daxiang XIANG received the B.S. and M.S. degrees in Remote Sensing from Wuhan University, Wuhan, Hubei province, China, in 2006 and 2008 respectively, where he is currently pursuing the Ph.D. degree. His primary research interest is the application of Remote Sensing in field of natural disaster monitoring.

Ming LI received the B.S. degree in GIS from China University of Geosciences, Wuhan, Hubei province, China, in 2008. Currently he is pursuing the Master degree in Wuhan University, Wuhan, Hubei province, China. His primary research interest is the application of Remote Sensing and GIS for natural disaster risk mapping.